This is a repository copy of *Dynamic avalanche free design in 1.2kV Si-IGBTs for ultra high current density operation*.

White Rose Research Online URL for this paper:
http://eprints.whiterose.ac.uk/153668/

Version: Accepted Version

Proceedings Paper:

Luo, P., Ekkanath Madathil, S.N., Nishizawa, S. et al. (1 more author) (2020) Dynamic avalanche free design in 1.2kV Si-IGBTs for ultra high current density operation. In: Proceedings of 2019 IEEE International Electron Devices Meeting (IEDM). 65th IEEE International Electron Devices Meeting (IEDM), 07-11 Dec 2019, San Francisco, CA, USA. Institute of Electrical and Electronics Engineers (IEEE) , 12.3.1-12.3.4. ISBN 9781728140339

https://doi.org/10.1109/IEDM19573.2019.8993596

© 2019 IEEE. Personal use of this material is permitted. Permission from IEEE must be obtained for all other users, including reprinting/ republishing this material for advertising or promotional purposes, creating new collective works for resale or redistribution to servers or lists, or reuse of any copyrighted components of this work in other works. Reproduced in accordance with the publisher's self-archiving policy.

Reuse

Items deposited in White Rose Research Online are protected by copyright, with all rights reserved unless indicated otherwise. They may be downloaded and/or printed for private study, or other acts as permitted by national copyright laws. The publisher or other rights holders may allow further reproduction and re-use of the full text version. This is indicated by the licence information on the White Rose Research Online record for the item.

Takedown

If you consider content in White Rose Research Online to be in breach of UK law, please notify us by emailing eprints@whiterose.ac.uk including the URL of the record and the reason for the withdrawal request.

eprints@whiterose.ac.uk
https://eprints.whiterose.ac.uk/

Dynamic Avalanche Free Design in 1.2kV Si-IGBTs for Ultra High Current Density Operation

Peng Luo[1], Sankara Narayanan Ekkanath Madathil[1], Shin-ichi Nishizawa[2], and Wataru Saito[2]
[1]Department of Electronic and Electrical Engineering, The University of Sheffield, U. K., email: pluo2@sheffield.ac.uk
[2]Research Institute for Applied Mechanics, Kyushu University, Fukuoka, Japan

Abstract**—**Dynamic Avalanche (DA) phenomenon poses a fundamental limit on the operating current density, turn-off power loss as well as reliability of MOS-bipolar devices. Overcoming this phenomenon is essential to ensure their safe operation in emerging electric transport. In this work, detailed analysis of 1.2 kV trench gated IGBTs are undertaken through experiments and calibrated TCAD simulations to show the fundamental cause of the DA as well as a method to achieve DA free design for ultra-high current density operation and reliability in 1.2 kV Si-IGBTs.

I. Introduction

Trench Gated Insulated Gate Bipolar Transistor (TIGBT) is a key component in power electronics applications today. More recently, new approaches to improve its performance by the enhancement of Injection Enhancement (IE) effect with narrow mesa and CMOS scaling rules have been reported [1]-[5]. The improvements in the switching loss (E_{off}) and on-state voltage drop ($V_{ce(sat)}$) trade-off have resulted in not only low loss operation but also increases in current density and improved cost performance of TIGBT modules. Low E_{off} (high dV/dt) can reduce the system size, because passive component can be shrunk with high frequency operation. However, high current density and high dV/dt during switching can induce DA [6]. TIGBTs have high concentrations of mobile carriers in the on-state, well above the background doping concentration. During turn-off, an increase in the potential drop occurs within a small space charge region of the device with a large part of stored carriers still present, as depicted in Figure 1. Dynamic avalanche (DA) will take place if the resulting electric field exceeds the critical electric field (E_{cr}), which can occur even at a voltage well below the static breakdown voltage. DA occurs in the vicinity of the trench gate and the generated charges due to Impact Ionization (I.I.) can have enough energy to be injected into the oxide thus degrading it and affecting reliability of the device [7]. Therefore, DA poses a fundamental limit on the operating current density, turn-off power loss [8] as well as reliability.

In this paper, an in-depth analysis of the TIGBT switching behavior focusing on the DA is presented through calibrated 3D TCAD models to show, for the first time, that removal of the high electric field concentration beneath the trench gates is the most important solution to manage the DA in TIGBTs. Moreover, for the first time, a DA free turn-off operation is demonstrated in a trench Clustered IGBT (TCIGBT) [9], through in both simulation and experiment. Moreover, the impact of device scaling design [1] on the DA is investigated in detail.

II. Dynamic Avalanche in TIGBTs

To analyze the DA in silicon TIGBTs, the 3D Sentaurus Device [10] is utilized to simulate the switching behavior, with a circuit configuration for mix-mode simulation as specified in Figure 2. The simulations were carried out at room temperature because the surge in voltage during turn-off is largely independent of the temperature [8]. The dependence of switch-off characteristics of a 1.2 kV TIGBT in Field-Stop (FS) technology on gate resistance (R_g) is shown in Figure 3. In practice, smaller R_g should induce large dV/dt; however, the DA decreases the dV/dt, which results in decrease in surge voltage even with small R_g conditions, as shown in Figure 3. This clearly indicates that DA occurs in the cases of R_g<20 Ω. In Figures 4(a) and (b) are shown a comparison of turn off curves, maximum electric fields (E_{max}) and maximum I.I. rates in the cases of R_g=0.1 Ω and R_g=50 Ω, respectively. In the case of R_g=0.1 Ω, due to DA, excessive holes created due to I.I. flow along the trench bottom because the peak electric field strength exceeds the critical value. Under large R_g conditions, the time to reach supply voltage takes longer, during which stored charges are removed and DA does not materialize. However, this comes at the expense of increased switching loss. Moreover, the saturation of E_{off} with Avalanche Generation (AG) model at small R_g conditions is due to the DA, as shown in Figure 5.

III. Danamic Avalanche Free Design: CIGBT

Recently, a new asymmetric gate oxide approach with a designed variable thickness to realise stable long-term operation in trench IGBTs and to reduce the switching delay and gate charge without sacrificing the electrical performance has been reported [11]. However, the DA phenomena cannot be suppressed in this design as well.

As a fundamental solution towards the DA suppression, TCIGBT is attractive because of its design for electric field management and does not suffer from DA as shown in Figure 5. Figure 6 shows the 3D cross-sectional view of a TCIGBT. The TCIGBT device features a MOS-gated thyristor structure, which consists of P-anode, N-drift, P-well and N-well. Its turn-on mechanism has been explained in [9]. During turn-off transient, due to the internal self-clamping feature of the TCIGBT, the N-well layer is punched through at collector voltages of less than 20 V and any further increase in voltage is supported by the P-well/N-well junction. Moreover, the inversion layers formed along the sidewall of trench gates connect the P-well layer with P-base region (PMOS). Such design provides a direct evacuation path for excess holes to be

collected within emitter region. The E_{off} is thus significantly reduced compared to a TIGBT structure, as shown in Figure 5.

Figures 7(a), (b) and (c) show a comparison of the electric field distributions, I.I. rates and hole densities at the time point of V_{ce} increases to 600 V between TIGBT and TCIGBT under R_g=0.1 Ω and identical $V_{ce(sat)}$ conditions, respectively. As can be seen, the trench gates of TCIGBT are protected from high electric field concentrations during turn-off. This is because, due to self-clamping, the potential of the N-well goes as high as the self-clamping voltage, thus turning on the PMOS formed between P well, N-well and P-base along the sidewall of the trench and the E_{max}, which is much less than E_{cr}, appears at the P-well/N-drift junction. However, in comparison, the TIGBT shows a strong electric field crowding in excess of the E_{cr} under the trench bottom and leads to a high I.I. rate.

Absence of the DA in TCIGBT is clearly evident from the experimental results of the switching waveforms of 1.2 kV, 40 Ampere devices measured as a function of R_g at different temperatures. For this purpose, a number of 8-Ampere devices fabricated using 6" wafers were connected in parallel as they have positive temperature coefficient of voltage. These devices show a $V_{ce(sat)}$ of less than 1.8 V at 140 A/cm^2 at room temperature and can support 1.6 kV and are short circuit proof [12]. Although the demonstrated devices were made in Non Punch-Through (NPT) technology, moving to a thinner FS technology has no impact on the DA, as discussed later. The differences in the slope of the surge voltage peak between the measured data in Figure 8 and in Figure 9 is mainly due to the parasitic capacitance in the measurement setup and has no impact on the DA. Figure 9(b) shows that TCIGBT does not show DA even at J_c=500 A/cm^2. This confirms that TCIGBT can be operated at ultra-high current density without DA and associated reliability concerns and with very low power losses.

IV. Impact of 3D Scaling on DA

To understand the impact of the 3D scaling on the DA performance of the devices, scaled TIGBTs [5] as well as scaled TCIGBTs [13] in FS technologies are considered, as shown in Figure 10 and Figure 12, respectively. The structures were evaluated through 3D modelling with models calibrated against measured data as shown in Figure 11. Note that the device thickness in all structures are identical as in [5] in order to compare the electrical characteristics. In Figure 13 is shown comparative *I-V* curves of *k3*-TIGBT and *k3*-TCIGBT under identical threshold voltage and same P-anode conditions. The *k3*-TCIGBT yields a low $V_{ce(sat)}$ of 1.67 V even at J_c=500 A/cm^2 and T_j=300 K, which is 23 % lower than that of *k3*-TIGBT. Furthermore, the non-saturated *I-V* behavior of narrow mesa TIGBTs is effectively suppressed in *k3*-TCIGBT due to enhanced self-clamping feature [13]. The E_{off} dependence on R_g between scaled TIGBTs and TCIGBTs were compared under same $V_{ce(sat)}$ conditions, as shown in Figure 14, which is achieved by adjusting P-anode concentration. The low switching losses of both devices decrease as a function of scaling rule. Moreover, the lower losses of *k3*-TCIGBT is clearly evident as shown in Figure 14 In TIGBT, 3D-scaling rule does not suppress DA, because enhanced IE effect influences are stronger than relaxation of electric field concentration as shown in Figure 15. However, as can be observed from Figure 14, *k3*-TIGBT does not show any obvious increase in E_{off}, which is due to fast hole evacuation by shallow trench. In any case, care must be taken to address reliability concerns with thinner gate oxides in TIGBTs.

The impact of the on-state carrier profile on DA in *k3*-TIGBT was analyzed by changing the resistance R_{pf} between the p-float region and the emitter, as shown in Figure 16(a). The carrier concentration at the emitter-side can be increased with high R_{pf} due to the IE effect. The rate of change of voltage is increased with decrease in R_{pf} (Figure 16(b)). Both I.I. rates and E_{max} values are enhanced by the positive charge of excess holes around the trench gate bottom (Figure 16(c)). Most importantly, these results shown in Figure 16 demonstrate that diversion of holes away from the trench bottom alone does not suppress DA. In Figures 17(a), (b) and (c) are shown some analysis of DA due to the increase in carrier concentration at the collector-side. Although the turn-off time can be increased by increasing P-anode concentration (Figure 17(b)), the collector-side carrier concentration has no influence on the DA (Figure 17(c)).

V. Conclusions

Dynamic Avalanche (DA) phenomenon poses a fundamental limit on the operating current density, turn-off power loss as well as reliability of MOS-bipolar devices. 1.2 kV trench IGBT switching behavior focusing on the DA was analyzed through calibrated 3D TCAD models for the first time. Management of the electric field concentration beneath trench gates is the most critical way to minimize the DA. In addition, a DA free turn-off operation is demonstrated in a trench Clustered IGBT (TCIGBT), through in both simulation and experiment. As a MOS controlled thyristor device, TCIGBT can be operated with very low power losses and at ultra-high current densities without DA and associated reliability concerns. This is because of the in-built self-clamping effect, which enhances PMOS behavior and reduction of electric field crowding at trench edges during turn-off. The impact of device scaling design on the DA has also been analyzed.

Acknowledgment

The authors thank the Japan Society for the Promotion of Science (JSPS) for support through an invitational fellowship. The authors also thank Prof. T. Hiramoto and his lab members for providing TIGBT experimental results.

References

[1] M. Tanaka and I. Omura, in *Proc. of ISPSD'12*, pp.177-180, 2012.
[2] K. Kakushima, et al., in *Tech Digest of IEDM'16*, pp. 10.6.1-10.6.4, 2016.
[3] C. Jaeger, et al., in *Proc. of ISPSD'17*, pp. 69-72, 2017.
[4] K. Eikyu, et al., in *Proc. of ISPSD'16*, pp. 211-214, 2016.
[5] T. Saraya et al., in Tech. *Digest of IEDM'18*, pp. 189-192, 2018.
[6] T. Ogura et al., *IEEE Trans., Electron Devices*, vol. 51, pp. 629-635, 2004.
[7] T. Laska, et al., *in Proc. of ISPSD'07*, pp. 1-4, 2007.
[8] S. Machida et al., in *Proc. of ISPSD'14*, pp. 107-110, 2014.
[9] O. Spulber et al., *IEEE Electron Device Lett*., vol. 21, pp. 613–615, 2000.
[10] *Sentaurus Device User Guide*: *Ver. L-2017.09*, 2017.
[11] C. Sandow et al., in *Proc. of ISPSD'18*, pp. 24-27, 2018.
[12] H. Long et al., in *Proc APEC*, pp. 1266-1269, 2015.
[13] P. Luo et al., *Trans., Electron Devices*, vol. 65(4), pp. 1440-1446, 2018.

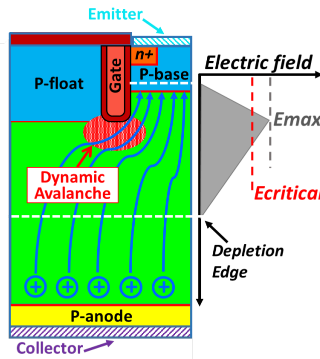

Figure 1. Schematic of dynamic avalanche in the turn-off transient of trench gated IGBT.

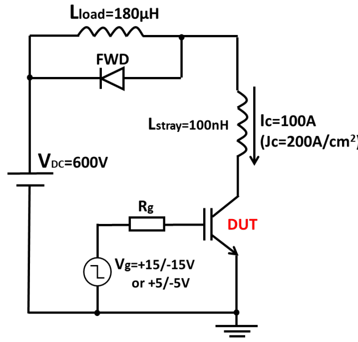

Figure 2. Test circuit configuration.

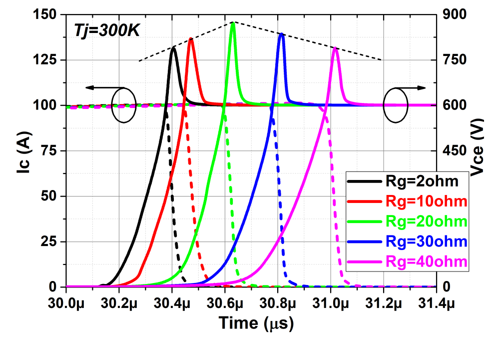

Figure 3. Switch-off characteristics of TIGBT at various R_g.

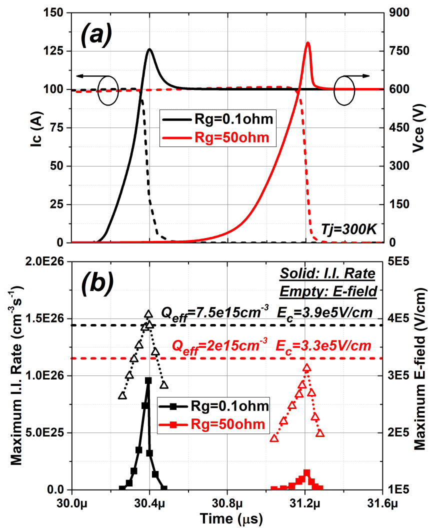

Figure 4. (a) Turn-off curves and (b) I.I. rates and E_{max} of a TIGBT at R_g=0.1Ω and 50Ω, respectively.

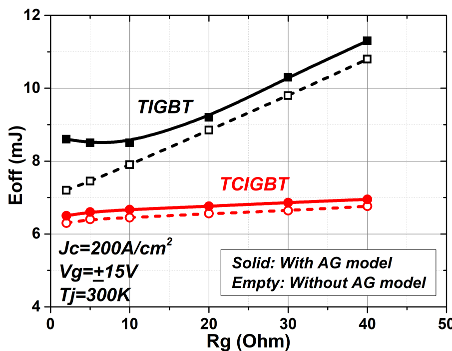

Figure 5. Dependence of E_{off} on R_g with AG model and without AG model, respectively.

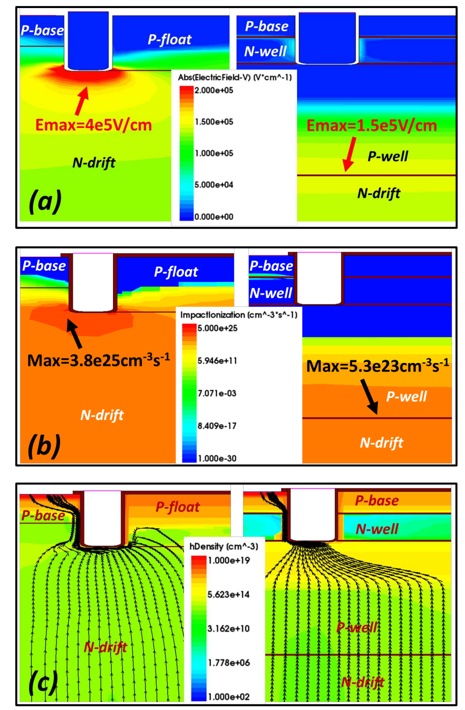

TIGBT TCIGBT
Figure 7. Comparison of (a) electric field distributions, (b) I.I. rate distributions and (c) hole densities when V_{ce} raises to 600V (R_g=0.1 Ω).

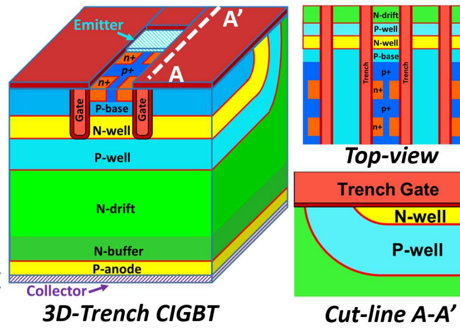

Figure 6. 3-D cross-sectional view of TCIGBT.

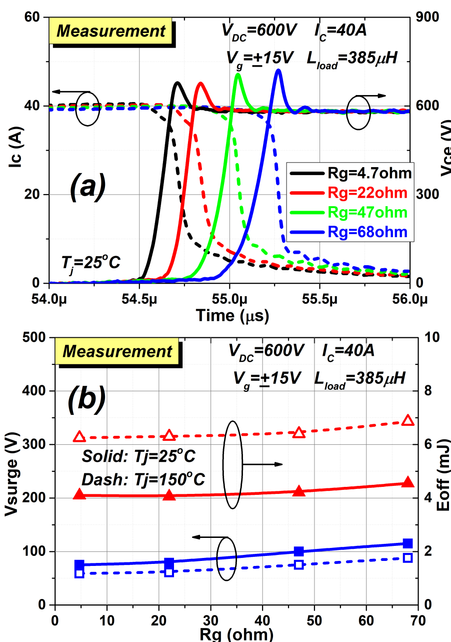

Figure 8. Experimental results of (a) turn-off curves and (b) surge voltage and E_{off} dependence on R_g of a 1.2kV, 40A TCIGBT in NPT technology.

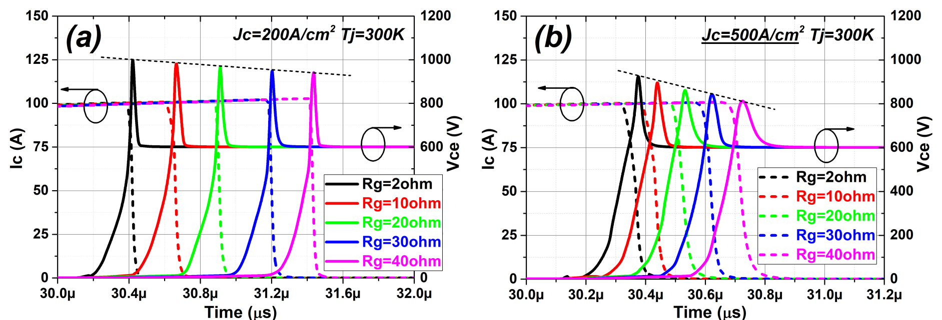

Figure 9. Simulated switch-off curves of TCIGBT at various R_g at (a) J_c=200A/cm² and (b) J_c=500A/cm².

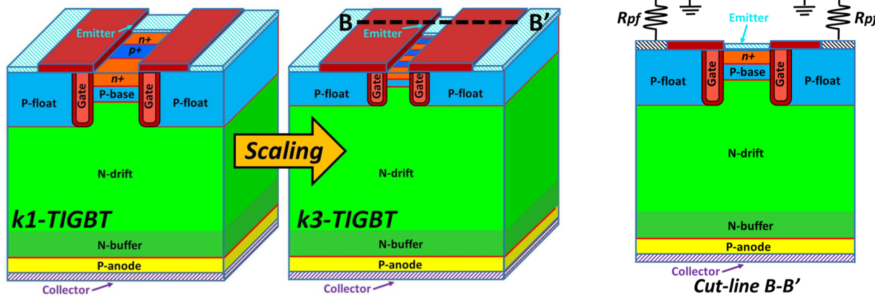

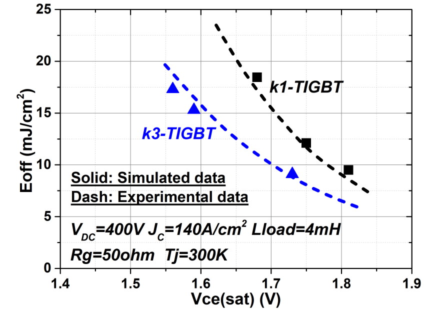

Figure 10. 3-D scaling rules of TIGBT [5]. Structural parameters are from [5]. P-float region is connected to emitter through a resistor.

Figure 11. Calibration of simulated models with experimental data in [5].

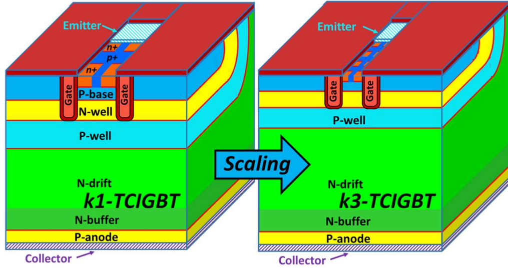

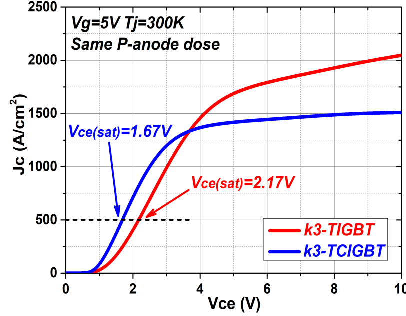

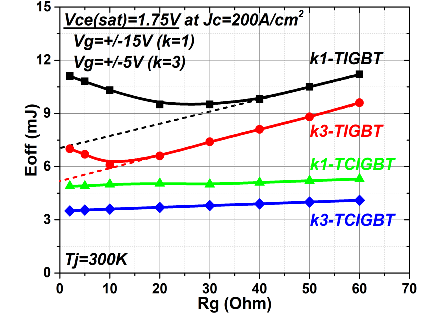

Figure 12. 3-D scaling rules of TCIGBT. Structural parameters of cathode cells are from [13].

Figure 13. Comparison of I-V characteristics between *k3*-TIGBT and *k3*-TCIGBT.

Figure 14. Impact of E_{off} versus R_g with scaling in TIGBTs and TCIGBTs under same $V_{ce(sat)}$ condition.

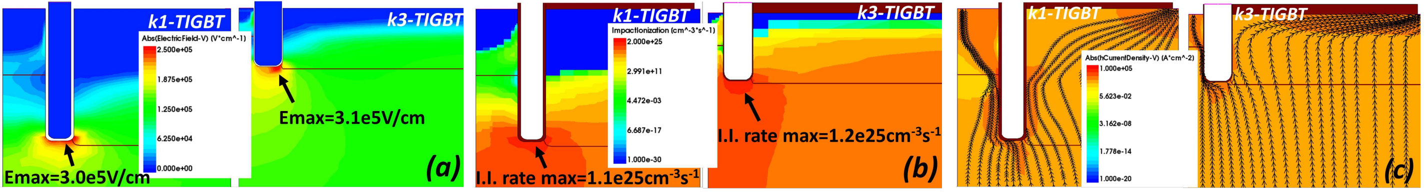

Figure 15. Comparison of (a) electric field distributions, (b) I.I. rates and (c) hole densities when V_{ce} raises to 600V between *k1*-TIGBT and *k3*-TIGBT (R_g=20 Ω).

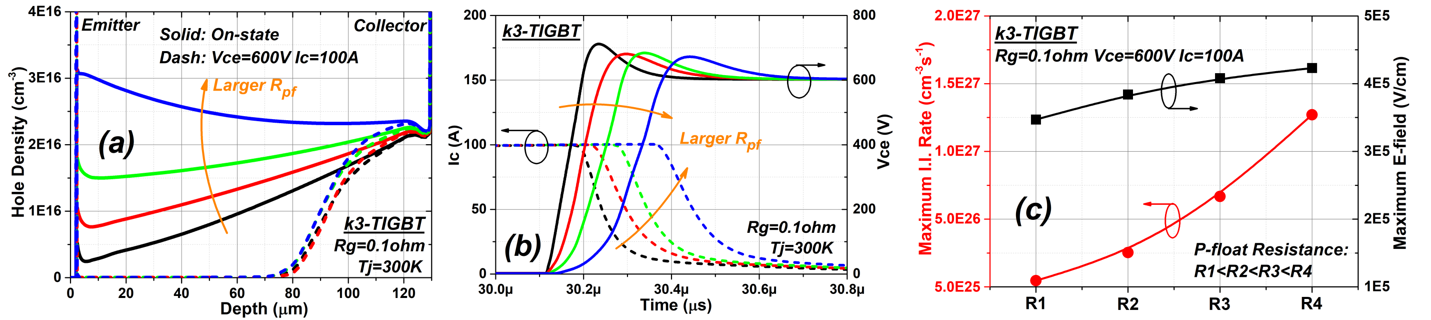

Figure 16. Influence of R_{pf} on (a) on-state hole density and excess hole density when V_{ce} raises to 600V, (b) switch-off characteristics, and (c) maximum electric field and maximum I.I. rate when V_{ce} raises to 600V in the case of *k3*-TIGBT. (V_g=+/-5V)

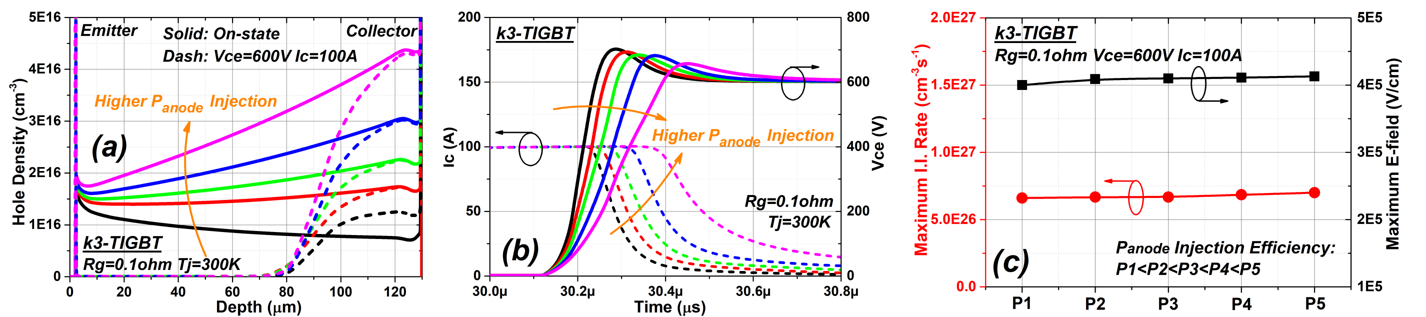

Figure 17. Influence of anode injection efficiency on (a) on-state hole density and excess hole density when V_{ce} raises to 600V, (b) switch-off characteristics, and (c) maximum electric field and maximum I.I. rate when V_{ce} raises to 600V in the case of *k3*-TIGBT. (V_g=+/-5V)